Online Optimal Active Sensing Control

Paolo Salaris, Riccardo Spica, Paolo Robuffo Giordano, Patrick Rives

Online Optimal Active Sensing Control

Paolo Salaris*, Riccardo Spica†, Paolo Robuffo Giordano† and Patrick Rives*

***Abstract*— This paper deals with the problem of active sensing control for nonlinear differentially flat systems. The objective is to improve the estimation accuracy of an observer by determining the inputs of the system that maximise the amount of information gathered by the outputs over a time horizon. In particular, we use the Observability Gramian (OG) to quantify the richness of the acquired information. First, we define a trajectory for the flat outputs of the system by using B-Spline curves. Then, we exploit an *online* gradient descent strategy to move the control points of the B-Spline in order to actively maximise the smallest eigenvalue of the OG over the whole planning horizon. While the system travels along its planned (optimized) trajectory, an Extended Kalman Filter (EKF) is used to estimate the system state. In order to keep *memory* of the past acquired sensory data for online re-planning, the OG is also computed on the past estimated state trajectories. This is then used for an online replanning of the optimal trajectory during the robot motion which is continuously refined by exploiting the state estimation obtained by the EKF. In order to show the effectiveness of our method we consider a simple but significant case of a planar robot with a single range measurement. The simulation results show that, along the optimal path, the EKF converges faster and provides a more accurate estimate than along other possible (non-optimal) paths.**

I. INTRODUCTION

The performance of robots and sensing devices is highly influenced by the quality and amount of sensor information, especially in case of limited sensing capabilities and/or low cost devices. Indeed, such information is often used to estimate the state of the system. As a consequence, the problem of optimal information gathering has been studied in the literature in a variety of contexts.

In the field of optimal sensor placements, in [1] an observability-based procedure is used to characterise the gyroscopic sensing distribution of the wings of the hawkmoth Manduca sexta. In [2] the problem of finding the optimal location of sensors on a wearable sensing glove was addressed in order to minimise the error statistics in the reconstruction of the hand pose.

In the field of localization and exploration for mobile robots, it is important to establish if, for a given system, the observation problem, that consists in finding an estimate of the state of the robot/environment from the knowledge of the inputs and the outputs over a period of time, admits a solution [3]. For instance, in [4] a complete observability analysis of the planar bearing-only localization and mapping problem for a nonholonomic vehicle and for all configurations of landmarks with known (markers) and unknown (targets) positions was studied by using the *Observability Rank Condition* (ORC) tool. The problem is shown to be *locally weakly observable* [5], if and only if the number of markers is equal or greater than two. For nonlinear systems, however, the observability may also depend on the inputs. In particular, for the above example, one can show the existence of *singular inputs* that do not allow the reconstruction of the state: this occurs with the vehicle aiming at the two markers or at the target directly.

The problem of developing intelligent control strategies applied to the data acquisition process [6] in order to maximise the amount of information coming from sensors, i.e. to maximise the "distance" from the singular trajectories, is an active area of research often known as *active sensing control*, *active perception* or *optimal information gathering*. One crucial point in this context is the choice of an appropriate *measure of observability* to optimise.

In [7] the condition number of the Observability Gramian (OG) is used as cost function to find the optimal observability trajectory for an Unmanned Aerial Vehicle (UAV) with GPS measurement and an Autonomous Underwater Vehicle (AUV) with range measurements from a single marker. One peculiarity of this work consists in finding an interesting relationship between the entries of the OG and the geometric properties of the trajectory, which can be useful to characterise the shape of the optimal path. In [8] the authors find optimal observability trajectories for first-order nonholonomic systems with nonholonomic states as outputs by maximising the smallest eigenvalue of the OG.

By using the concept of entropy, introduced by Shannon, the authors of [9] devised an observability measure and an optimal navigation strategy for a unicycle vehicle with three bearing measurements w.r.t. known markers. The problem of finding informative paths in Gaussian fields has also been tackled in [10], where the authors propose to maximise a cost function based on the concept of mutual information between the state and the measurements. In [11], a Bayesian optimisation approach for determining the most informative path is used. A search based method for planning in information space was developed in [12] to provide an adaptive policy for mobile sensors with non-linear sensing models. In [13], the optimal trajectories for a team of robots moving on a plane and tracking a target by using relative measurements (distances and bearings) were obtained by minimising the trace of the target's position estimate covariance matrix under suitable constraints.

In the field of simultaneous localization and mapping (SLAM), [14] presents sub-optimal paths that minimise an adaptively weighted combination of the uncertainty of the vehicle pose and of the map features. In [15], a trajectory

* are with INRIA Sophia-Antipolis Méditerranée, 2004 Route des Lucioles, 06902 Sophia Antipolis, France, e-mail: psalaris,prives@inria.fr. † are with the CNRS at Irisa and Inria Rennes Bretagne Atlantique, Campus de Beaulieu, 35042 Rennes Cedex, France, e-mail: riccardo.spica,prg@irisa.fr.

optimisation for target localization by using 3D bearing-only measurements from small unmanned aerial vehicles is proposed. The active sensing problem consists in minimising the trace of the inverse of the Fisher Information Matrix (FIM). Similarly, in [16], the objective is to find the best trajectories and camera configurations for a group of aerial Dubins vehicles, equipped with Pan-Tilt-Zoom cameras, that maximise the trace of the information matrix of the Extended Information Filter (EIF) used for estimating the position of a target on the ground.

Because of the difficulty of the problem only few papers tried to tackle active sensing control from an analytic point of view. In [17], the effects of observer motion on estimation accuracy for bearing-only measurements was addressed. In [18], the problem of maximising the smallest eigenvalue of the OG was casted within the calculus of variation theory ([19]) and solved for a flat 2D system with only one output measurement.

In this paper, we consider a differentiable approximation of the smallest eigenvalue of the OG (i.e. the Schatten norm) as a measure of observability in order to avoid the non-differentiability in case of repeated eigenvalues. The originality of our method is that it combines an *online* gradient-descent optimization strategy with a concurrent estimation scheme (an Extended Kalman Filter in our case) meant to recover an estimation of the true (but unknown) state during motion. The need for an *online* solution is motivated by the fact that, for a nonlinear system, the observability Gramian is a function of the state trajectories, which, in a real scenario, are not assumed available. By using an offline optimisation method that relies on the initial estimation, the resulting trajectory would be sub-optimal – e.g. in a worst-case scenario of a system that admits singular inputs, the optimal trajectory from the estimated initial position may be the singular one from the real initial position.

In order to make the online optimisation problem tractable from an optimisation point of view, we restrict our attention to the case of non-linear differentially flat systems [20] and we represent the flat outputs with a family of curves (B-Spline) function of a finite number of parameters. To check the effectiveness of our method we will consider a planar robot with a single nonlinear output measurement (the squared distance from a marker) for which a partial analytic solution can also be obtained by applying the results in [18] (see the Appendix in [21]) — an analytic analysis that can serve as a 'ground truth' for validating the results of the proposed gradient-based method (which can, instead, be applied to any differentially flat system and output map for which an analytic analysis may not be possible).

We believe that the formulation of our problem is quite general and the computational efficiency and simplicity of the proposed solution allow applying it to more complex systems than the one considered in this paper as a case study, as, e.g. unicycles and quadrotor UAVs. Moreover, the method can be further generalised by including the environment (e.g. targets) as state variables to be estimated and by introducing additional constraints in order to, e.g., avoid obstacles or reach points of interest.

The paper is structured as follows. In Section II the optimal control problem is introduced while in Section III a solution that combines an online gradient-descent optimization strategy with a concurrent estimation scheme is provided. In Section IV we apply our method to a flat 2D system. Finally, the paper ends with some conclusions.

II. PROBLEM STATEMENT

Let us consider a generic nonlinear dynamics

$$\dot{\boldsymbol{q}}(t) = \boldsymbol{f}(\boldsymbol{q}(t), \boldsymbol{u}(t)), \quad \boldsymbol{q}(t_0) = q_0 \tag{1}$$

$$\boldsymbol{z}(t) = \boldsymbol{h}(\boldsymbol{q}(t)) + \boldsymbol{\nu} \tag{2}$$

where $\boldsymbol{q}(t) \in \mathbb{R}^n$ represents the state of the system, $\boldsymbol{u}(t) \in \mathcal{U}$ is the control input ($\mathcal{U}$ is a subset of $\mathbb{R}^m$), $\boldsymbol{z}(t) \in \mathbb{R}^p$ is the sensor output (the measurements available through the onboard sensors), $\boldsymbol{f}$ and $\boldsymbol{h}$ are analytic functions and $\nu \sim \mathcal{N}(0, R(t))$ is a normally-distributed Gaussian output noise with zero mean and covariance matrix $\boldsymbol{R}(t)$ A well-known observability criterion for system (1)–(2), related to the concept of local *indistinguishable* states [3], [18], is the *Observability Gramian* (OG) $\boldsymbol{\mathcal{G}}_o(t_0, t_f) \in \mathbb{R}^{n\times n}$:

$$\boldsymbol{\mathcal{G}}_o(t_0, t_f) \triangleq \int_{t_0}^{t_f} \boldsymbol{\Phi}(\tau, t_0)^T \boldsymbol{H}(\tau)^T \boldsymbol{W}(\tau) \boldsymbol{H}(\tau) \boldsymbol{\Phi}(\tau, t_0)\, \mathrm{d}\tau \tag{3}$$

where $t_f > t_0$, $\boldsymbol{H}(\tau) = \frac{\partial \boldsymbol{h}(\boldsymbol{q}(\tau))}{\partial \boldsymbol{q}(\tau)}$, and $\boldsymbol{W}(\tau) \in \mathbb{R}^{p\times p}$ is a symmetric positive definite weight matrix (a design parameter), that may be used for, e.g. accounting for outputs with different units and/or, as in this paper, for considering the reliability of the outputs with different noise levels. Matrix $\boldsymbol{\Phi}(t, t_0) \in \mathbb{R}^{n\times n}$, also known as *sensitivity matrix*, is given as $\boldsymbol{\Phi}(t, t_0) = \frac{\partial \boldsymbol{q}(t)}{\partial \boldsymbol{q}_o}$ and verifies the following differential equation

$$\dot{\boldsymbol{\Phi}}(t, t_0) = \frac{\partial f(\boldsymbol{q}(t), \boldsymbol{u}(t))}{\partial \boldsymbol{q}(t)} \boldsymbol{\Phi}(t, t_0)\,, \qquad \boldsymbol{\Phi}(t_0, t_0) = I. \tag{4}$$

If the (symmetric and positive definite) matrix $\boldsymbol{\mathcal{G}}_o$ is full rank over the time interval $[t_0,\, t_f]$, then system (1)–(2) is *locally weakly observable*, i.e. it is possible to (locally) recover the state trajectory $\boldsymbol{q}(t)$ from the knowledge of $\boldsymbol{z}(t)$ and $\boldsymbol{u}(t)$, $t \in [t_0,\, t_f]$. The OG, similarly to the well-known Observability Rank (OR) condition [5], can hence be exploited for verifying the observability of a given nonlinear system. However, while the OR condition can only provide a "binary answer" about the observability of the system, the OG also provides a measure of the amount of information gathered by the sensors along the trajectory followed during motion [22]. One can then attempt maximization of some performance index of the OG (typically a function of its eigenvalues) w.r.t. the system inputs in order to produce a system trajectory with maximum information content over a future time horizon.

In this paper, we will consider the smallest eigenvalue of the OG as performance index, i.e. $\lambda_{min}\left(\boldsymbol{\mathcal{G}}_o(t_0, t_f)\right)$, and we will determine the optimal control strategy $\boldsymbol{u}^*(t)$, $t \in [t_0,\, t_f]$ that maximises $\lambda_{min}\left(\boldsymbol{\mathcal{G}}_o(t_0, t_f)\right)$. Indeed, the inverse of the

smallest eigenvalue of the OG is proportional to the maximum estimation uncertainty, and hence, its *maximisation* is expected to *minimize* the maximum estimation uncertainty of any estimation strategy that could be used, e.g. a EKF [8]. By increasing the value of the smallest eigenvalue, we also expect the convergence rate of the observer to increase. However, it is well-known that considering the smallest eigenvalue of a matrix $\boldsymbol{A}$ as a cost function can be ill-conditioned from a numerical point of view in case of repeated eigenvalues. For this reason, as also done in [23], we will consider the following cost function (aka Schatten norm),

$$\|\boldsymbol{A}\|_\mu = \sqrt[\mu]{\sum_{i=1}^{n} \lambda_i^\mu(\boldsymbol{A})} \tag{5}$$

with $\mu \ll -1$, as a differentiable approximation of $\lambda_{min}(\boldsymbol{A})$. Moreover, to ensue well-possness of the optimisation problem, we will constrain the solution to be such that the "control effort" (or energy) needed by the robot for moving along the trajectory from t_0 to t_f is fixed and equal to $\bar{E}$, i.e.

$$E(t_0, t_f) = \int_{t_0}^{t_f} \sqrt{\boldsymbol{u}(\tau)^T \boldsymbol{M} \boldsymbol{u}(\tau)}\, \mathrm{d}\tau = \bar{E}\,.^1 \tag{6}$$

The rest of the paper is hence devoted to propose an *online* solution to our problem that will combine an online gradient-descent optimization strategy with a concurrent estimation scheme (an EKF in our case) meant to recover an estimation $\hat{\boldsymbol{q}}(t)$ of the true (but unknown) state $\boldsymbol{q}(t)$ during motion. The need for an *online* solution is motivated as follows: the Gramian $\boldsymbol{\mathcal{G}}_o$ is a function of the whole state trajectory $\boldsymbol{q}(t)$, $t \in [t_0,\, t_f]$, but the state and, in particular, the initial condition $\boldsymbol{q}(t_0)$, is not assumed available. Therefore, in order to perform an offline optimization of $\boldsymbol{\mathcal{G}}_o$, one would necessarily need to rely on some estimated $\hat{\boldsymbol{q}}(t)$ (for example, by integrating the system dynamics from an initial estimation $\hat{\boldsymbol{q}}(t_0)$). Since $\hat{\boldsymbol{q}}(t)$ is only an approximation of the true state evolution $\boldsymbol{q}(t)$, the resulting optimized path would then represent, in general, a sub-optimal one. On the other hand, during the robot motion, it is possible to exploit a state estimation algorithm, such as a EKF, for improving *online* the current estimation $\hat{\boldsymbol{q}}(t)$ of the true state $\boldsymbol{q}(t)$, with $\hat{\boldsymbol{q}}(t) \to \boldsymbol{q}(t)$ in the limit. Availability of a converging state estimation $\hat{\boldsymbol{q}}(t)$ then makes it possible to continuously refine (online) the previously optimised path by leveraging the newly acquired information during motion.

Before presenting our proposed solution in the next Section, we conclude with three remarks.

Remark 1 *In general, a closed-form expression for the sensitivity matrix $\boldsymbol{\Phi}$ may not be available, since finding a solution for* (4) *is as complex as finding a solution for* (1)*. However, in some particular cases of interest (e.g. the unicycle) matrix $\boldsymbol{\Phi}$ can be found in closed form. For all the other cases, a numerical integration of (4) is required.*

Remark 2 *The* integrand *in* (3) *can have full rank only if $p \geq n$, i.e. if the number of available measurements is larger or equal than the number of state variables (such as, for instance, in Structure from Motion (SfM) problems [24]). When $p < n$ (as in the case studies reported in Sections IV), maximization of λ_{min} (or of its differentiable approximation) is still possible but only in an integral sense (i.e. over the whole time horizon T) as shown in the reported results.*

Remark 3 *The method we propose in this paper can be used not only with the OG but also with other measures of information, as e.g. the Kalman filter/smoother covariance matrix, related to the mutual information, or the Fisher information matrix. A sensible conclusion is that all these measures are related and hence the obtained solutions should be similar. Future works will be dedicated to determine an analytical relationship of equivalency between all these measures.*

III. AN ONLINE GRADIENT-BASED SOLUTION TO ACTIVE SENSING CONTROL

We assume, as explained before, that a EKF is run by the robot during its motion for producing an estimation $\hat{\boldsymbol{q}}(t)$ (and associated estimated covariance matrix $\hat{\boldsymbol{P}}(t)$) from the collected measurements and applied inputs. Let $\bar{t} \in [t_0, t_f]$ be a generic time instant during the robot motion and partition (3) as

$$\boldsymbol{\mathcal{G}}_o(t_0, t_f) = \boldsymbol{\mathcal{G}}_o(t_0, \bar{t}) + \boldsymbol{\mathcal{G}}_o(\bar{t}, t_f)\,. \tag{7}$$

The first term $\boldsymbol{\mathcal{G}}_o(t_0, \bar{t})$ represents a "memory" of the past information already collected via the available measurements during $t \in [t_0,\, \bar{t}]$ and can be computed by numerically integrating (3) along the past estimated trajectory. This term is obviously constant and cannot be optimised any longer at time $t = \bar{t}$. On the other hand, the second term $\boldsymbol{\mathcal{G}}_o(\bar{t}, t_f)$ represents the information yet to be collected during $t \in [\bar{t},\, t_f]$ that can, instead, still be optimised.

We note that, although the term $\boldsymbol{\mathcal{G}}_o(t_0, \bar{t})$ is a constant parameter w.r.t. the optimization variables, one still needs to include it in the cost function since in general $\lambda_{min}(\boldsymbol{A} + \boldsymbol{B}) \geq \lambda_{min}(\boldsymbol{A}) + \lambda_{min}(\boldsymbol{B})$ (Weyl's inequality). Furthermore, as explained, both terms in (7) are function of the state evolution $\boldsymbol{q}(t)$ which is assumed unknown: therefore, $\boldsymbol{\mathcal{G}}_o(t_0, \bar{t})$ must be evaluated on the estimated state trajectory $\hat{\boldsymbol{q}}(t)$, $t \in [t_0,\, \bar{t}]$, and $\boldsymbol{\mathcal{G}}_o(\bar{t}, t_f)$ on a "predicted" state trajectory generated from the current $\hat{\boldsymbol{q}}(\bar{t})$.

In order to make the problem more tractable from an optimization point of view (and, thus, to better cope with the real-time constraint of an online implementation) we now make two simplifying working assumptions. First, we restrict our attention to the case of non-linear differentially flat[2] systems [20]: as well-known, for these systems one

[1]Indeed, in general $\lambda_{min}\left(\boldsymbol{\mathcal{G}}_o(t_0, t_f)\right)$ could be unbounded from above without the control effort E.

[2]The class of flat systems includes some of the most common robotic platforms such as, e.g. unicycles, cars with trailers and quadrotor UAVs, and in general any system which can be (dynamically) feedback linearized [25].

can find a set of outputs $\boldsymbol{\zeta} \in \mathbb{R}^m$, termed *flat*, such that the state and inputs of the original system can be expressed *algebraically* in terms of these outputs and a finite number of their derivatives. In the context of this work, the differentially flatness assumption allows avoiding the numerical integration of the nonlinear dynamics (1) for generating the future state evolution $\hat{\boldsymbol{q}}(t)$, $t \in [\bar{t}, t_f]$, from the planned inputs $\boldsymbol{u}(t)$ and the current state estimate $\hat{\boldsymbol{q}}(\bar{t})$. Second, we represent the flat outputs (and, as a consequence, also the state and inputs of the considered system) with a family of parametric curves. This assumption allows then reducing the complexity of the problem from an infinite-dimensional optimization into a finite-dimensional one.

Among the many possibilities, and taking inspiration from [26], in this work we leverage the family of B-Splines [27] as parametric curves. B-Spline curves are linear combinations, through a *finite* number of control points $\mathbf{x}_c = (\mathbf{x}_{c,1}^T,\ \mathbf{x}_{c,2}^T,\ \ldots,\ \mathbf{x}_{c,N}^T)^T \in \mathbb{R}^m \cdot N$, of basis functions $B_j^\lambda : S \to \mathbb{R}$ for $j = 1, \ldots, N$. Each B-Spline is given as

$$\begin{aligned} &\gamma(\mathbf{x}_c, \cdot) : S \to \mathbb{R}^m \\ &\qquad s \mapsto \sum_{j=1}^{N} \mathbf{x}_{c,j}\, B_j^\alpha(\mathbf{s}, s) = \mathbf{B}_\mathbf{s}(s)\mathbf{x}_c \end{aligned} \tag{8}$$

where S is a compact subset of $\mathbb{R}$, $\mathbf{B}_\mathbf{s}(s) \in \mathbb{R}^{m \times N}$. The degree $\alpha > 0$ and knots $\mathbf{s} = (s_1,\ s_2,\ \ldots,\ s_\ell)$ are constant parameters[3]. $\mathbf{B}_\mathbf{s}(s)$ is the collection of basis functions and B_j^α is the *j*-th basis function evaluated in s, obtained by means of the Cox-de Boor recursion formula [27]. In the following, the control points $\mathbf{x}_c$ will hence become the optimization variables.

Notice that the value $s(t)$ of the parameter s corresponding to the time t depends on the desired timing law along the path. Without loss of generality, in the following we will assume that an arc-length parametrization is used, and hence $s(t)$ can be simply computed by integrating $\dot{s}(t) = v(\mathbf{x}_c, s)^{-1}$ where $s(t)$ is the value of parameter s corresponding to the path length t.

We are now able to state the online optimal active sensing control problem expressed in terms of B-Splines.

Problem 1 (On-line active sensing control via B-Spline) *Given the non linear system* (1)–(2)*, an estimation $\hat{\boldsymbol{q}}(\bar{t})$ of the true state $\boldsymbol{q}(\bar{t})$ at time $\bar{t}$ with covariance matrix $\boldsymbol{P}(\bar{t})$ and a time horizon $T - \bar{t} = t_f - t_o - \bar{t} > 0$, find the optimal position of the control points $\mathbf{x}_c^*$ such that,*

$$\mathbf{x}_c^* = \arg\max_{\mathbf{x}_c}\ \|\boldsymbol{\mathcal{G}}_o(t_0, \bar{t}) + \boldsymbol{\mathcal{G}}_o(\mathbf{x}_c, s)\|_\mu \tag{9}$$

where

$$\boldsymbol{\mathcal{G}}_o(\mathbf{x}_c, s) = \int_{s(\bar{t})}^{s(t_f)} \boldsymbol{Q}^T(\mathbf{x}_c, \sigma)\boldsymbol{R}^{-1}\boldsymbol{Q}(\mathbf{x}_c, \sigma)\ v(\mathbf{x}_c, \sigma)\mathrm{d}\sigma$$

[3] The relation between ℓ, α and N is $\ell = N - \alpha + 1$. α is chosen in order to guarantee the continuity of all the state variables that, in turns, depend on the flat outputs and a finite number of their derivatives. Once this property is guaranteed, both α and N can be chosen as a trade-off between the computational cost and the possibility of obtaining a better trajectory (increasing the value of the smallest eigenvalue of the OG).

and such that

$$\int_{s(\bar{t})}^{s(t_f)} \sqrt{\boldsymbol{u}(\mathbf{x}_c, \sigma)^T \boldsymbol{M} \boldsymbol{u}(\mathbf{x}_c, \sigma)}\mathrm{d}\sigma = \bar{E} - E(t_0, \bar{t}) \tag{10}$$

where M is a constant weight matrix and $\bar{E}$ is a constant design parameter. Moreover

$$\begin{aligned} \boldsymbol{Q}(\mathbf{x}_c, \sigma) &= \frac{\partial \boldsymbol{h}(\boldsymbol{q})}{\partial \boldsymbol{q}} \boldsymbol{\Phi}(\mathbf{x}_c, \sigma)\,, \\ \boldsymbol{\mathcal{G}}_o(t_0, \bar{t}) &= \int_{t_0}^{\bar{t}} \boldsymbol{\Phi}(\tau, t_0)^T \frac{\partial \boldsymbol{h}(\boldsymbol{q}(\tau))}{\partial \boldsymbol{q}(\tau)}^T \boldsymbol{R}^{-1} \frac{\partial \boldsymbol{h}(\boldsymbol{q}(\tau))}{\partial \boldsymbol{q}(\tau)} \boldsymbol{\Phi}(\tau, t_0)\mathrm{d}\tau, \\ E(t_0, \bar{t}) &= \int_{s(t_0)}^{s(\bar{t})} \sqrt{\boldsymbol{u}(\mathbf{x}_c, \sigma)^T \boldsymbol{M} \boldsymbol{u}(\mathbf{x}_c, \sigma)}\, \mathrm{d}\sigma\,. \\ v(\mathbf{x}_c, \sigma) &= \left\| \frac{\partial \gamma(\mathbf{x}_c, \sigma)}{\partial s} \right\|_2 . \end{aligned}$$

We then now proceed to detail our proposed solution to Problem 1, under the stated assumptions, which will consist in a gradient-based action affecting the location of the control points $\mathbf{x}_c$ and, thus, the overall shape of the trajectory followed by the system.

It is important to note that in (9) only the integral over the time interval $[\bar{t}, t_f]$ depends on the positions of the control points. The same applies for the computation of (10).

Problem 1 can be solved by adopting an online gradient-descent optimization strategy. We introduce a time dependency $\mathbf{x}_c(t)$ so that the B-Spline path becomes a time varying path. Moreover, we assume that the control points move according to the following simple update law

$$\dot{\mathbf{x}}_c(t) = \boldsymbol{u}_c(t), \qquad \mathbf{x}_c(t_0) = \boldsymbol{x}_{c,0}\,, \tag{11}$$

where $\boldsymbol{u}_c(t) \in \mathbb{R}^m \times N$.

Remark 4 *During motion, while the observer is updating $\hat{\boldsymbol{q}}(\bar{t})$, it is also important to guarantee that the B-Spline curves, which define the future state trajectories, pass through the current state $\hat{\boldsymbol{q}}(\bar{t})$ at time $\bar{t}$. Indeed, $\hat{\boldsymbol{q}}(\bar{t})$ depends on the update law of the EKF and is independent from the B-Spline shaping due to the gradient-descent optimisation strategy. Once this constraint is satisfied, the control point movements, due to the gradient of the cost functional in* (9)*, while also guaranteeing the control effort constraint, must not violate this requirement. Further local properties at time $\bar{t}$ may have to be guaranteed during control point movements. This imposes some continuity constraints on the flat outputs at $\bar{t}$ and some of their derivatives (those affecting the system state) which, in turn, results in additional constraints on the motion of the B-Splines coefficients.*

The gradient update rule for the control points that solves Problem 1 while guaranteeing Remark 4 can be generated online as

$$\boldsymbol{u}_c(\bar{t}) = \boldsymbol{u}_{\hat{q}}(\bar{t}) + \mathrm{Nu}_C\left(\boldsymbol{u}_E(\bar{t}) + \mathrm{Nu}_E \nabla_{\mathbf{x}_c} \|\boldsymbol{\mathcal{G}}_o\|_\mu\right) \tag{12}$$

In (12), the term $\boldsymbol{u}_{\hat{q}}$ guarantees that $\boldsymbol{e}_{\hat{q}}(\bar{t}) = \boldsymbol{q}_\gamma(\gamma(\mathbf{x}_c(\bar{t}), s(\bar{t})), \dot{\gamma}(\mathbf{x}_c(\bar{t}), s(\bar{t})), \ldots) - \hat{\boldsymbol{q}}(\bar{t}) \equiv 0$, i.e. realises the first requirement of Remark 4. Indeed, since

$$\dot{\gamma}(\mathbf{x}_c(t), s(t)) = \frac{\partial \boldsymbol{q}_\gamma(\gamma(\mathbf{x}_c(t), s(t)))}{\partial s}\dot{s}(t) + \frac{\partial \boldsymbol{q}_\gamma(\gamma(\mathbf{x}_c(t), s(t)))}{\partial \mathbf{x}_c}\boldsymbol{u}_c(t)$$

one has

$$\boldsymbol{u}_{\hat{q}} = -\boldsymbol{J}_{\gamma}^{\dagger}\left(K_{\hat{q}}\boldsymbol{e}_{\hat{q}}(\bar{t}) + \left.\frac{\partial \boldsymbol{q}_{\gamma}(\gamma(\mathbf{x}_c(t),s(t)))}{\partial s}\right|_{\mathbf{x}_c(\bar{t}),s(\bar{t})}\dot{s}(\bar{t})\right)$$

where, $\boldsymbol{J}_{\gamma} = \left.\frac{\boldsymbol{q}_{\gamma}(\gamma(\mathbf{x}_c(t),s(t)))}{\partial \mathbf{x}_c}\right|_{\mathbf{x}_c(\bar{t}),s(\bar{t})}$ and $K_{\hat{q}}$ is a constant parameter. On the other hand, matrix $\mathrm{Nu}_C = I_{2N} - \boldsymbol{J}_C^{\dagger}\boldsymbol{J}_C$ is the projector onto the null space of

$$\boldsymbol{J}_C = \left[\frac{\partial\gamma(\mathbf{x}_c,s)}{\partial\mathbf{x}_c},\ \frac{\partial}{\partial s}\frac{\partial\gamma(\mathbf{x}_c,s)}{\partial\mathbf{x}_c},\ \cdots,\ \frac{\partial^{(k)}}{\partial s^{(k)}}\frac{\partial\gamma(\mathbf{x}_c,s)}{\partial\mathbf{x}_c}\right]_{\mathbf{x}_c(\bar{t}),s(\bar{t})}$$

This projector guarantees that the requirement of maximising the smallest eigenvalue of OG while maintaining $E(\bar{t},t_f) = \bar{E} - E(t_0,\bar{t})$ can be accomplished without changing the primary task $\boldsymbol{e}_{\hat{q}}(\bar{t}) \equiv 0$, hence realising the second requirement of Remark 4, and also other local properties at $\gamma(\mathbf{x}_c(\bar{t}),s(\bar{t}))$ of the B-Spline, as e.g. the tangency, the curvature, and so on. For instance, if some nonholonomic constraints must be satisfied for the nonlinear system, the tangency at $\gamma(\mathbf{x}_c(\bar{t}),s(\bar{t}))$ must not be influenced by the movement of the control points, and matrix Nu_C would be exploited for enforcing this constraint.

The term $\boldsymbol{u}_E(\bar{t})$ is designed so as to guarantee the control effort constraint, i.e. $e_E(\bar{t}) = E(\bar{t},t_f) - (\bar{E} - E(t_0,\bar{t})) \equiv 0$, where $E(t_0,\bar{t})$ at time $\bar{t}$ is considered a constant since it cannot be modified any longer by moving the control points. As a consequence,

$$\boldsymbol{u}_E(\bar{t}) = -K_E\boldsymbol{J}_E e_E(\bar{t})\,,$$

where

$$\boldsymbol{J}_E = \int_{s(\bar{t})}^{s(t_f)} \frac{\partial\sqrt{\boldsymbol{u}(\mathbf{x}_c,\sigma)^T\boldsymbol{M}\boldsymbol{u}(\mathbf{x}_c,\sigma)}}{\partial\mathbf{x}_c}\mathrm{d}\sigma.$$

Matrix $\mathrm{Nu}_E = I_{2N} - \boldsymbol{J}_E^{\dagger}\boldsymbol{J}_E$ is the projector onto the null space of $\boldsymbol{J}_E$. It guarantees that $\nabla_{\mathbf{x}_c}\|\boldsymbol{\mathcal{G}}_o\|_{\mu}$ does not affect the control effort constraint. Finally,

$$\nabla_{\mathbf{x}_c}\|\boldsymbol{\mathcal{G}}_o\|_{\mu} = \sqrt[\frac{1-\mu}{\mu}]{\sum_{i=1}^{n}\lambda_i^{\mu}(\boldsymbol{\mathcal{G}}_o)}\sum_{i=1}^{n}\mu\lambda_i^{\mu-1}(\boldsymbol{\mathcal{G}}_o)\mathrm{v}_i^T\frac{\partial\boldsymbol{\mathcal{G}}_o}{\partial\mathbf{x}_c}\mathrm{v}_i$$

where, v_i is the eigenvector associated to the eigenvalue λ_i and

$$\frac{\partial\boldsymbol{\mathcal{G}}_o}{\partial\mathbf{x}_c} = \int_{s(\bar{t})}^{s(t_f)}\frac{\partial\boldsymbol{Q}^T(\mathbf{x}_c,\sigma)\boldsymbol{R}^{-1}\boldsymbol{Q}(\mathbf{x}_c,\sigma)\,v(\mathbf{x}_c,\sigma)}{\partial\mathbf{x}_c}\mathrm{d}\sigma$$

IV. SIMULATION RESULTS

In order to prove the effectiveness of our optimal active sensing control strategy, in this section we apply the proposed method to a planar robot that needs to estimate its position by using, as its only output, the squared distance from the origin of a fixed global reference frame. The objective here is is to determine the most informative trajectory, i.e. the trajectory that, by limiting the control effort to be $\bar{E}$, maximizes the smallest eigenvalue of the OG and hence reduces as much as possible the maximum estimation uncertainty. Let us hence consider the following dynamic system

$$\begin{cases}\dot{x}(t) = u_x(t)\\ \dot{y}(t) = u_y(t)\\ z(t) = h(x(t),y(t)) + \nu\,,\end{cases} \tag{13}$$

that represents a planar robot with position $\boldsymbol{q}(t) = [x(t),\ y(t)]^T$. The quantity $\nu \sim \mathcal{N}(0,R)$ is the output noise and $R \in \mathbb{R}$ is the constant variance of ν. We will consider as output of the system the squared distance, hereafter named *range*, w.r.t. a marker located at the origin of a global reference frame

$$z(t) = h(\boldsymbol{q}(t)) + \nu = x(t)^2 + y(t)^2 + \nu\,. \tag{14}$$

The sensitivity matrix $\boldsymbol{\Phi}(t,t_0) = I$ for (13) while $\frac{\partial h(\boldsymbol{q})}{\partial\boldsymbol{q}} = 2[x(t),\ y(t)]$. As a consequence, the OG is given by

$$\boldsymbol{\mathcal{G}}_o(t_0,t_f) = \int_{t_0}^{t_f} 4R^{-1}\begin{bmatrix}x(\tau)^2 & x(\tau)y(\tau)\\ x(\tau)y(\tau) & y(\tau)^2\end{bmatrix}\mathrm{d}\tau \tag{15}$$

With $\boldsymbol{M} = I$, the control effort constraint in Problem 1 is exactly the length of the path that, without loss of generality, the vehicle follows at constant speed equal to 1. The N control points that define the path are 2D points, i.e. $\mathbf{x}_c \in \mathbb{R}^2$, i.e. $m = n$, and $\boldsymbol{p}(t) = \gamma(\mathbf{x}_c(t),s(t)) \in \mathbb{R}^2$ is the planar trajectory of the robot. In order to improve the estimation of the position of the system, we will use, as explained, a EKF as state estimation algorithm.

As a consequence, the optimal control problem for (13) with output (14) consists in determining the path of length $\bar{E} \equiv T$ that maximise the smallest eigenvalue of the OG. The solution to this problem can be obtained by applying the control law given by (12) to the control points.

Fig. 1 compares the estimation performance of a EKF filter when the system moves either along a straight line path, or along the optimal path obtained by solving Problem 1 for the considered system[4]. Moreover, in Table I all data and numerical results are also reported. It is important to point out that, once an estimation of the robot initial position is available, the optimal path from this position is obtained (the green line path in Fig. 1, upper right corner) starting from an initial guess that, in our simulation, coincides with the straight line path used for the comparison. Of course, given the non convexity of the considered optimisation problem, the initial guess will determine towards which local minimum the algorithm will converge. Global optimization procedures (which could, e.g. iterate over a number of different initial guesses) can clearly be adopted. However, for the sake of space, this analysis is omitted in this paper and left to future developments. Interestingly, however, we have heuristically verified that the dynamic system considered in this section is not very sensible to this choice.

At the very first iteration, the vehicle only starts moving once the control points have reached their optimal configuration, and hence an optimal B-Spline path is obtained for the current estimated position. Note that, due to estimation

[4]A video of the simulation is also attached to the paper.

TABLE I

NUMERICAL SIMULATION RESULTS OF FIG. 1. FOR BOTH SIMULATIONS, THE VEHICLE STARTS FROM $\boldsymbol{q}(t_0) = [1.41,\ 1.41]^T$ [M] AND THE INITIAL ESTIMATION IS $\hat{\boldsymbol{q}}(t_0) = [1.11,\ 1.91]^T$ [M] WITH $\boldsymbol{P}_o = 0.5\, I$. THE INITIAL ESTIMATION ERROR IS $\boldsymbol{e}(t_0) = [0.3,\ 0.5]^T$. THE CONTROL EFFORT ALONG THE PATH THAT IN THIS CASE COINCIDES WITH THE LENGTH OF THE PATH IS FOR BOTH CASES $E(t_0, t_f) = 5.64$ [M]. THE OUTPUT NOISE COVARIANCE MATRIX $R = 3 \cdot 10^{-1}$. THE NUMBER OF CONTROL POINTS $N = 5$ AND THE DEGREE OF THE B-SPLINE $\alpha = 3$. NOTICE THAT THE EIGENVALUES ARE COMPUTED TO LESS THAN R.

	$\boldsymbol{q}(t_f)$ [m]	$\hat{\boldsymbol{q}}(t_f)$ [m]	$\boldsymbol{e}(t_f)$ [m]$\times 10^{-2}$	$RMS(\boldsymbol{e}(t_f))$	$\lambda_{min}(\boldsymbol{\mathcal{G}}_o(t_f))$	$\lambda_{MAX}(\boldsymbol{\mathcal{G}}_o(t_f))$
Optimal path	$x(t_f) = 0.80$ $y(t_f) = -2.86$	$\hat{x}(t_f) = 0.81$ $\hat{y}(t_f) = -2.84$	$e_x(t_f) = -1.56$ $e_y(t_f) = -2.69$	$2.20 \cdot 10^{-2}$	58.33	50.41
Straight line path	$x(t_f) = 7.05$ $y(t_f) = 1.41$	$\hat{x}(t_f) = 7.03$ $\hat{y}(t_f) = 1.50$	$e_x(t_f) = 2.57$ $e_y(t_f) = -9.04$	$6.65 \cdot 10^{-2}$	11.03	501.29

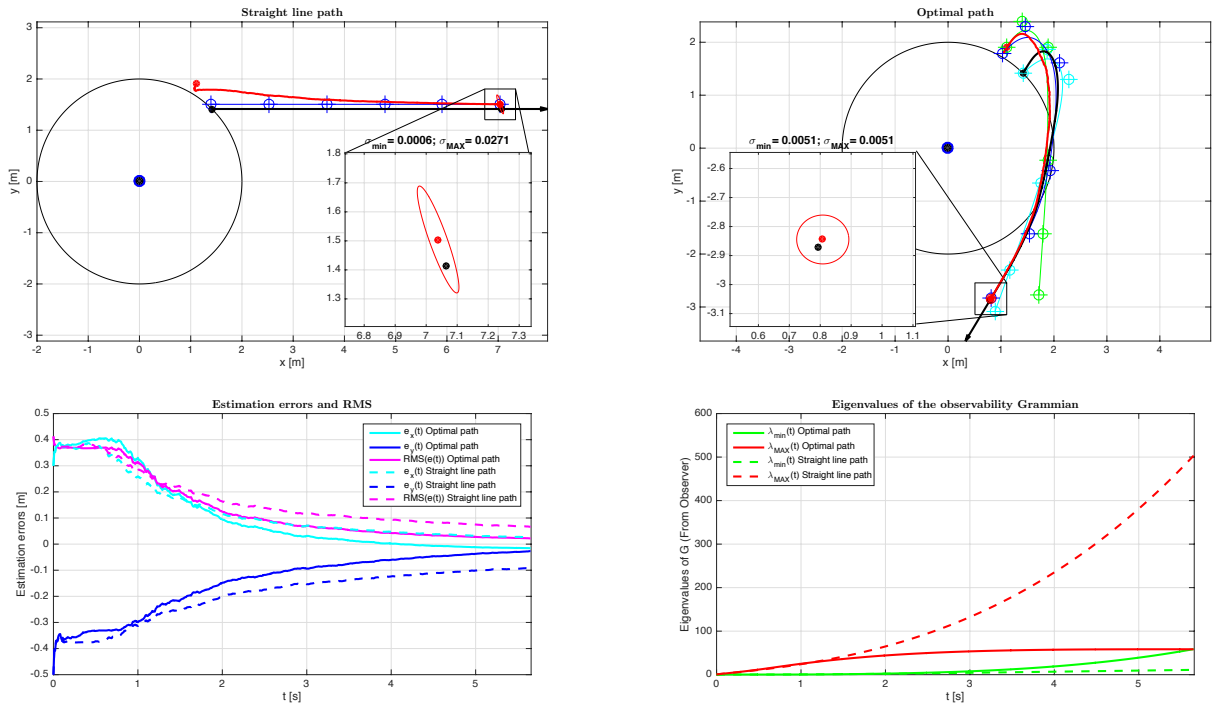

Fig. 1. The estimation performance with the EKF along the optimal path is compared with a simple straight line path (it coincides with the initial guess for the optimization procedure). At the end of the optimal path the smallest eigenvalue reaches a value that is double w.r.t. the one reached at the end of the straight line path. Moreover, the eigenvalues almost coalesce at the end of the optimal path (they do not reach exactly also the same value because of the use of the Schatten norm). Notice that the eigenvalues are computed to less than R. Along the optimal path the rms of the estimation error reaches a smaller value and the error ellipse is uniformly shaped and smaller than along the straight line path. As a consequence, the active sensing control gives rise to a more precise and accurate estimation.

errors, this path might be sub-optimal. However, while the robot moves along the planned path, the EKF reduces the estimation error and the gradient descent strategy keeps updating *online* the shape of the optimal path. As a consequence, the final B-Spline path will, in general, differ from the one computed at the beginning (compare the blue line path with the green one, in Fig. 1, upper right corner) because of the better estimated state provided by the EKF during motion. In Fig. 1, upper right corner, the real robot trajectory and the estimated one are also reported in black and red lines, respectively. For completeness, also the optimal path from the real initial position of the robot is reported in cyan.

Notice that until 1 s of simulation, the straight line path outperforms the optimal one in terms of convergence rate to zero of the RMS of the estimation error (see Fig. 1, in the bottom left side). Indeed, the optimal path starts along a direction that is almost unobservable, i.e. almost tangent to the straight line passing through the origin and the initial position of the system. It is clear that along this first part of the optimal path the smallest eigenvalue has a negligible increase, giving rise to poor information. However, once the system changes direction and aligns to the second part of the path, the smallest eigenvalue increases rapidly until it reaches the maximum value which is almost equal to the largest eigenvalue. Indeed, at the end, along the optimal path the RMS of the estimation error is three times smaller than the one reached along the straight line path. This demonstrates the fundamental non-local nature of the observability property, expressed by means of the smallest eigenvalue of OG for which, obviously, $\lambda_{min}(\boldsymbol{A} + \boldsymbol{B}) \neq \lambda_{min}(\boldsymbol{A}) + \lambda_{min}(\boldsymbol{B})$.

The estimation uncertainty ellipses at the end of each

path are also reported. Since, along the optimal path, the smallest eigenvalue of OG is maximised, the ellipse is much less elongated along the eigenvector associated to the largest eigenvalue of the covariance matrix. As a consequence, along the optimal path, a more precise and accurate estimation can be obtained. Moreover, as the observation time is enough for the smallest eigenvalue to reach the value of the largest one (see Fig. 1, in the bottom right corner), the estimation uncertainty ellipse is almost a circle and hence a uniform estimation uncertainty is obtained.

V. CONCLUSIONS AND FUTURE WORKS

In this paper, the problem of active sensing control for non-linear differentially flat systems has been tackled. The smallest eigenvalue of the observability Gramian has been used to quantify the richness of the acquired information. Then, we have represented the flat outputs with a family of B-Spline whose shape can be adjusted by changing a finite number of parameters. We hence have exploited an *online* gradient descent strategy to move the control points of such B-Spline in order to actively maximise the smallest eigenvalue of the OG, while at the same time, an Extended Kalman Filter (EKF) has been used to estimate the system state. By applying our strategy to a planar robot, we have shown that with an EKF the maximum estimation uncertainty and the convergence rate is significantly reduced along the optimal path, thus giving rise to an improved estimation of the state at the end of the path.

Future works will mainly consist in applying the proposed method to more complex systems as e.g. unicycles and quadrotors with multiples markers and different kinds of measurements. The problem will be also extended to multiple robot systems. An important step towards the use of our method in SLAM problems is to include the environment within the state of variable to be estimated. It would be then interesting to observe the differences between the optimal trajectories obtained in case of targets and in case of markers at the same position. As a final point, it will be important to address Remark 3.

REFERENCES

[1] B. T. Hinson and K. A. Morgansen, "Gyroscopic sensing in the wings of the hawkmoth manduca sexta : the role of sensor location and directional sensitivity," *Bioinspiration & Biomimetics*, vol. 10, no. 5, p. 056013, 2015.

[2] M. Bianchi, P. Salaris, and A. Bicchi, "Synergy-based hand pose sensing: Optimal glove design," *International Journal of Robotics Research (IJRR)*, vol. 32, no. 4, pp. 407–424, April 2013, impact factor: 2.523, 5-Year Impact factor: 3.206.

[3] G. Besançon, *Nonlinear observers and applications*. Springer, 2007, vol. 363.

[4] F. A. Belo, P. Salaris, D. Fontanelli, and A. Bicchi, "A complete observability analysis of the planar bearing localization and mapping for visual servoing with known camera velocities," *International Journal of Advanced Robotic Systems*, vol. 10, 2013.

[5] R. Hermann and A. J. Krener, "Nonlinear controllability and observability," *IEEE Transactions on automatic control*, vol. 22, no. 5, pp. 728–740, 1977.

[6] R. Bajcsy, "Active perception," *Proceedings of the IEEE*, vol. 76, no. 8, pp. 966–1005, Aug. 1988.

[7] B. T. Hinson, M. K. Binder, and K. A. Morgansen, "Path planning to optimize observability in a planar uniform flow field," in *American Control Conference (ACC)*, June 2013, pp. 1392–1399.

[8] B. T. Hinson and K. A. Morgansen, "Observability optimization for the nonholonomic integrator," in *American Control Conference (ACC)*, June 2013, pp. 4257–4262.

[9] J. Shan and Q. Sun, "Observability analysis and optimal information gathering of mobile robot navigation system," in *IEEE International Conference on Information and Automation*, Aug 2015, pp. 731–736.

[10] J. L. Ny and G. J. Pappas, "On trajectory optimization for active sensing in gaussian process models," in *Proceedings of the 48th IEEE Conference on Decision and Control (CDC), held jointly with the 28th Chinese Control Conference (CCC).*, Dec 2009, pp. 6286–6292.

[11] R. Marchant and F. Ramos, "Bayesian Optimisation for informative continuous path planning," in *IEEE International Conference on Robotics and Automation (ICRA)*. IEEE, 2014, pp. 6136–6143.

[12] N. Atanasov, J. Le Ny, K. Daniilidis, and G. J. Pappas, "Information acquisition with sensing robots: Algorithms and error bounds," in *IEEE International Conference on Robotics and Automation (ICRA)*. IEEE, 2014, pp. 6447–6454.

[13] K. Zhou and S. I. Roumeliotis, "Multirobot Active Target Tracking With Combinations of Relative Observations," *IEEE Transactions on Robotics*, vol. 27, no. 4, pp. 678–695, 2011.

[14] F. Bourgault, A. A. Makarenko, S. B. Williams, B. Grocholsky, and H. F. Durrant-Whyte, "Information based adaptive robotic exploration," in *IEEE/RSJ International Conference on Intelligent Robots and Systems (IROS)*, vol. 1, Oct. 2002, pp. 540–545 vol.1.

[15] S. Ponda, R. Kolacinski, and E. Frazzoli, "Trajectory Optimization for Target Localization Using Small Unmanned Aerial Vehicles," in *AIAA Guidance, Navigation, and Control Conference*. Reston, Virigina: American Institute of Aeronautics and Astronautics, Jun. 2012.

[16] C. Ding, A. A. Morye, J. A. Farrell, and A. K. Roy-Chowdhury, "Coordinated sensing and tracking for mobile camera platforms," in *American Control Conference (ACC)*, June 2012, pp. 5114–5119.

[17] S. E. Hammel, P. T. Liu, E. J. Hilliard, and K. F. Gong, "Optimal observer motion for localization with bearing measurements," *Computers & Mathematics with Applications*, vol. 18, no. 1-3, pp. 171–180, Jan. 1989.

[18] F. Lorussi, A. Marigo, and A. Bicchi, "Optimal exploratory paths for a mobile rover," in *IEEE International Conference on Robotics and Automation (ICRA)*, vol. 2, 2001, pp. 2078–2083.

[19] I. Gelfand and S. Fomin, *Calculus of variations*. Courier Corporation, 2000, translated and edited by R. A. Silverman.

[20] M. Fliess, J. Lévine, P. Martin, and P. Rouchon, "Flatness and defect of nonlinear systems: Introductory theory and examples," *International Journal of Control*, vol. 61, no. 6, pp. 1327–1361, 1995.

[21] P. Salaris, R. Spica, P. Robuffo Giordano, and P. Rives, "Online Optimal Active Sensing Control," in *International Conference on Robotics and Automation (ICRA)*, Singapore, Singapore, May 2017. [Online]. Available: https://hal.inria.fr/hal-01472608

[22] A. J. Krener and K. Ide, "Measures of unobservability," in *Proceedings of the 48th IEEE Conference on Decision and Control, held jointly with the 28th Chinese Control Conference. CDC/CCC*, Dec 2009, pp. 6401–6406.

[23] R. Spica and P. Robuffo Giordano, "Active decentralized scale estimation for bearing-based localization," in *IEEE/RSJ International Conference on Intelligent Robots and Systems (IROS)*, October 2016.

[24] R. Spica, P. R. Giordano, and F. Chaumette, "Active structure from motion: Application to point, sphere, and cylinder," *IEEE Transactions on Robotics*, vol. 30, no. 6, pp. 1499–1513, Dec 2014.

[25] A. D. Luca and G. Oriolo, "Trajectory planning and control for planar robots with passive last joint," *International Journal of Robotics Research (IJRR)*, vol. 21, no. 5–6, pp. 575–590, 2002.

[26] C. Masone, P. R. Giordano, H. H. Blthoff, and A. Franchi, "Semi-autonomous trajectory generation for mobile robots with integral haptic shared control," in *IEEE International Conference on Robotics and Automation (ICRA)*, May 2014, pp. 6468–6475.

[27] L. Biagiotti and C. Melchiorri, *Trajectory planning for automatic machines and robots*. Springer Science & Business Media, 2008.

APPENDIX
ANALYTIC SOLUTION ANALYSIS FOR THE FLAT 2D SYSTEM

By applying the results of [18] to the planar robot used in Section IV with range output measurement, the analytic optimal solution can be partially obtained for

Problem 2 (Active sensing control) *Given the nonlinear system* (1)–(2)*, an initial condition* $q(t_0)$ *and a time horizon* $T = t_f - t_0 > 0$*, find the optimal control strategy* $u^*(t)$*,* $t \in [t_0,\, t_f]$*,*

$$u^*(t) = \arg\max_u \ \lambda_{min}\left(\mathcal{G}_o(t_0, t_f)\right), \quad (16)$$

$$s.t.$$

$$E(t_0, t_f) = \int_{t_0}^{t_f} \sqrt{u(\tau)^T M u(\tau)}\, \mathrm{d}\tau = \bar{E} \quad (17)$$

where M *is a constant weight matrix and* $\bar{E}$ *is a constant design parameter.*

For the sake of space, we will not provide a summary of the results reported in [18] and we refer the reader to the paper for details about the analytic procedure.

The observability Gramian is given by (15) and the smallest eigenvalue from $t_0 = 0$ and $t_f = T$ is

$$\lambda_{min} = \frac{1}{2}\int_0^T h_x^2 + h_y^2 \mathrm{d}t + \\ - \frac{1}{2}\sqrt{\left(\int_0^T h_x^2 - h_y^2 \mathrm{d}t\right)^2 + 4\left(\int_0^T h_x h_y \mathrm{d}t\right)^2}. \quad (18)$$

The extremal of the optimal control Problem 2, i.e. the curve that satisfies the necessary conditions for optimality, is

$$y(t) - y_0 = \pm m(x(t) - x_0) \quad (19)$$

which is the equation of a straight line passing through the initial position $q(t_0) = (x(t_0), y(t_0)) = (x_0, y_0)$, with slope m. An arc-length parametrization for (19) is

$$x(t) = \pm\frac{t}{\sqrt{1+m^2}} + x_0 \quad (20)$$

$$y(t) = -\frac{m\, t}{\sqrt{1+m^2}} + y_0\,. \quad (21)$$

By substituting the above parametric equations in (18) and deriving with respect to m, we obtain extremals corresponding to values of m (i.e. the slope of the straight line) that solve $\frac{\partial \lambda_{min}(\mathcal{G}_o)}{\partial m} = 0$. It is possible to identify two distinct values. The first one, which corresponds to $\lambda_{min}(\mathcal{G}_o) = 0$, is $m^{min}_{\lambda_{min}} = \frac{y_0}{x_0}$, i.e. a straight line passing through $q(t_0)$ and the origin of the marker (see the red line in Fig. 2).

The second solution $m^{max}_{\lambda_{min}}$ corresponds to a maximum of $\lambda_{min}(\mathcal{G}_o)$

$$m^* = \frac{4x_0y_0 - T\sqrt{4\left(x_0^2 + y_0^2\right) - T^2}}{T^2 - 4y_0^2}\,. \quad (22)$$

and it is valid for $0 \leq T \leq (3x_0 - \sqrt{3}y_0)\sqrt{\frac{x_0^2+y_0^2}{3x_0^2 - 2\sqrt{3}x_0y_0 + y_0^2}} = \bar{T}$ where $\bar{T}$ is the minimum length path from which the two eigenvalues coalesce. As a consequence, for path length T smaller or equal than $\bar{T}$ the optimal path is a segment from $q(t_0)$ to the circumference centered at the origin and passing through $q(t_0)$.

For any path longer than $\bar{T}$, the maximum of the smallest eigenvalue is reached when the two eigenvalues coalesce.

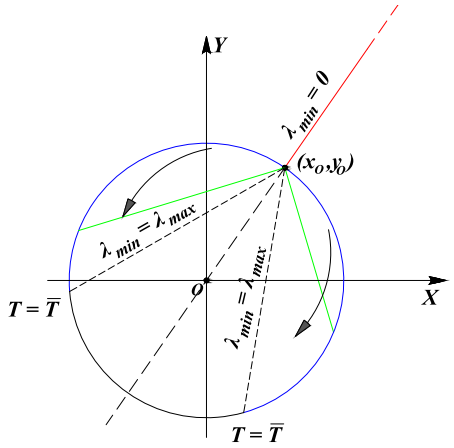

Fig. 2. Optimal path for the flat 2D system in case of the available time horizon $0 \leq T \leq \bar{T}$.

However, the first derivative of the smallest eigenvalue at these optimal values does not exist – the smallest eigenvalue function is not differentiable. For this reason, the above method can not be applied to find the optimal solution for path whose length is longer than $\bar{T}$ and hence different methods should be used [**?**].

Remark 5 *The trace of the observability Gramian for the 2D system with range as a measurement is* $trace(\mathcal{G}) = \int_0^T x^2(t) + y^2(t)dt$*, i.e. the integral of the output during the time. It is clear that this integral is maximised by moving as far as possible from the origin and it is minimised by approaching as much as possible the origin. Both conditions can be reached along a straight line passing through the origin. However, along both paths, the smallest eigenvalue is zero. A similar behaviour can be obtained by using the determinant of the Gramian. This example explains why we prefer to use the smallest eigenvalue as measure of observability.*

To verify that the optimal solution provided by our method coincides with the one obtained with the analytic procedure until path length $\bar{T}$ and to complete the solution set for $T > \bar{T}$, in Fig. 3, several B-Spline paths with different lengths that solve Problem 2 are reported by assuming that the initial position of the system is known. To avoid the non differentiability of the smallest eigenvalue in case of the smallest eigenvalues coalesce, the Schatten norm is used with $p \ll 0$. The degree of the B-Spline basis is $\lambda = 2$ while the number of control points is $n = 3$. The first control point coincides with the initial position of the system and hence is fixed. A greater number of control points and a larger degree can be use do not give a significant improvement. Notice that, for any optimal path in the picture, there exists the symmetric one, w.r.t. the straight line passing through the origin and the initial position of the system, which is also optimal. It is interesting to note for lengths $T > \bar{T}$, the optimal path is no longer a straight line and the smallest eigenvalue can increase until the eigenvalues of the Gramian almost coalesce. Moreover, the paths begin

along a direction that is almost unobservable, i.e. almost tangent to the straight line passing through the origin and the initial position of the system. It is clear that, along this first part of the path the smallest eigenvalue has a negligible increase, giving rise to poor information. However, once the system changes direction and aligns to the second part of the path, which tends to a straight line, the smallest eigenvalue increases rapidly until it reaches the maximum value which is almost equal to the largest eigenvalue. This enlightens the fundamental non local nature of the observability property which, however, can be correctly tackled by our proposed method.

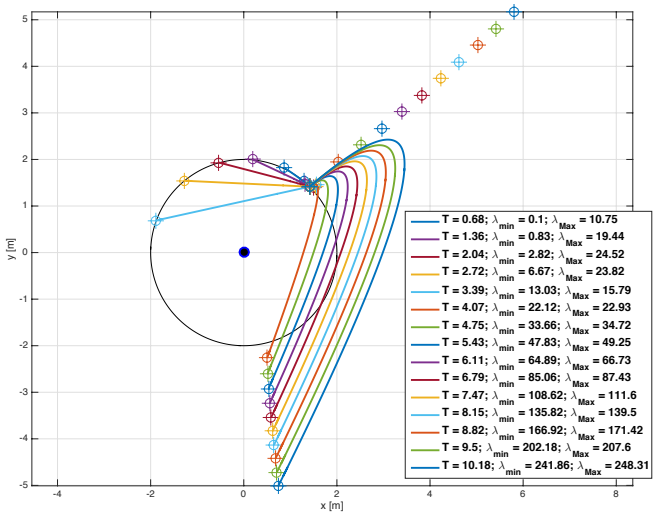

Fig. 3. Several optimal arc-length parametrised paths for different lengths T for the flat 2D system with range output measurement. The initial position is $(\sqrt{2}, \sqrt{2})$, the number of control points for each path is $n = 3$, the degree of the B-Spline is $\lambda = 2$ the measure of observability is the Schatten norm.